

## Correlations between the strange quark condensate, strange quark mass, and kaon PCAC relation

D. Harnett<sup>1,\*</sup>, J. Ho<sup>2,†</sup> and T. G. Steele<sup>3,‡</sup>

<sup>1</sup>*Department of Physics, University of the Fraser Valley, Abbotsford, British Columbia V2S 7M8, Canada*

<sup>2</sup>*Department of Physics, Dordt University, Sioux Center, Iowa 51250, USA*

<sup>3</sup>*Department of Physics and Engineering Physics, University of Saskatchewan, Saskatoon, Saskatchewan S7N 5E2, Canada*



(Received 22 April 2021; accepted 5 May 2021; published 4 June 2021)

Correlations between the strange quark mass, strange quark condensate  $\langle \bar{s}s \rangle$ , and the kaon partially conserved axial current (PCAC) relation are developed. The key dimensionless and renormalization-group invariant quantities in these correlations are the ratio of the strange to nonstrange quark mass  $r_m = m_s/m_q$ , the condensate ratio  $r_c = \langle \bar{s}s \rangle / \langle \bar{q}q \rangle$ , and the kaon PCAC deviation parameter  $r_p = -m_s \langle \bar{s}s + \bar{q}q \rangle / 2f_K^2 m_K^2$ . The correlations define a self-consistent trajectory in the  $\{r_m, r_c, r_p\}$  parameter space constraining strange quark parameters that can be used to assess the compatibility of different predictions of these parameters. Combining the constraint with Particle Data Group (PDG) values of  $r_m$  results in  $\{r_c, r_p\}$  constraint trajectories that are used to assess the self-consistency of various theoretical determinations of  $\{r_c, r_p\}$ . The most precise determinations of  $r_c$  and  $r_p$  are shown to be mutually consistent with the constraint trajectories and provide improved bounds on  $r_p$ . In general, the constraint trajectories combined with  $r_c$  determinations tend to provide more accurate bounds on  $r_p$  than direct determinations. The  $\{r_c, r_p\}$  correlations provide a natural identification of a self-consistent set of strange quark mass and strange quark condensate parameters.

DOI: [10.1103/PhysRevD.103.114005](https://doi.org/10.1103/PhysRevD.103.114005)

QCD sum-rules techniques probe hadronic properties via QCD composite operators with appropriate quantum numbers and quark/gluonic valence content to serve as interpolating fields for hadronic states [1,2] (for reviews, see e.g., Refs. [3–5]). Correlation functions of these composite operators are calculated from QCD using the operator-product expansion and are then related to hadronic properties through dispersion relations, which are converted to a QCD sum rule through application of an appropriate transform. Important features of these correlation functions are the power-law corrections induced by QCD condensates (vacuum expectations values) that parametrize non-perturbative aspects of the QCD vacuum.

In QCD sum-rules analyses of hadronic systems containing strange quarks, the strange quark mass  $m_s$ , and the

strange quark condensate  $\langle \bar{s}s \rangle$  are important parameters. Depending upon the system, the condensate may emerge as  $\langle \bar{s}s \rangle$  or be accompanied with quark mass factors (e.g.,  $m_s \langle \bar{s}s \rangle$ ,  $m_c \langle \bar{s}s \rangle$ ). However,  $\langle \bar{s}s \rangle$  is also used within determinations of higher-dimension condensates, including the vacuum-saturation approximation for dimension-six quark condensates and the dimension-five mixed condensate [6,7]

$$\langle g\bar{s}\sigma_{\mu\nu}\lambda^a G_{\mu\nu}^a s \rangle = \langle g\bar{s}\sigma G s \rangle = ((0.8 \pm 0.1) \text{ GeV}^2) \langle \bar{s}s \rangle. \quad (1)$$

Because of these multiple roles in determining different QCD condensates, the strange quark condensate is an essential parameter in QCD sum rules and provides insight into  $SU(3)$  flavor symmetry of the QCD vacuum.

QCD sum-rules studies of the strange quark condensate are based upon pseudoscalar and scalar correlation functions combined with low-energy theorems (see e.g., Refs. [8–10])

$$\begin{aligned} \Psi_5(q^2) &= i \int d^4x \langle \Omega | T(J_5(x) J_5^\dagger(0)) | \Omega \rangle, \\ J_5(x) &= i(m_u + m_s) \bar{s}(x) \gamma_5 u(x), \end{aligned} \quad (2)$$

$$\Psi_5(0) = -(m_s + m_u) \langle \bar{s}s + \bar{q}q \rangle, \quad (3)$$

\*derek.harnett@ufv.ca

†jason.ho@dordt.edu

‡tom.steele@usask.ca

Published by the American Physical Society under the terms of the [Creative Commons Attribution 4.0 International license](https://creativecommons.org/licenses/by/4.0/). Further distribution of this work must maintain attribution to the author(s) and the published article's title, journal citation, and DOI. Funded by SCOAP<sup>3</sup>.

$$\Psi(q^2) = i \int d^4x \langle \Omega | T(J(x)J^\dagger(0)) | \Omega \rangle, \quad (4)$$

$$J(x) = i(m_s - m_u)\bar{s}(x)u(x),$$

$$\Psi(0) = -(m_s - m_u)\langle \bar{s}s - \bar{q}q \rangle, \quad (5)$$

where  $SU(2)$  isospin symmetry of the vacuum implies  $\langle \bar{q}q \rangle = \langle \bar{u}u \rangle = \langle \bar{d}d \rangle$ .

QCD sum-rules determinations of the low-energy constants  $\Psi_5(0)$  and  $\Psi(0)$  contain  $\langle \bar{s}s \rangle$  dependence and thus provide a natural means to extract the strange quark condensate (see e.g., Refs. [8,9]). For example, the ratio  $\Psi_5(0)/\Psi(0)$  can be used to reference the strange quark condensate to the nonstrange condensate through the renormalization-group (RG) invariant ratio and the RG invariant strange quark mass ratio  $\xi = m_u/m_s = 0.024 \pm 0.006 \ll 1$  [11]

$$\frac{\Psi_5(0)}{\Psi(0)} = \left( \frac{1 + \xi}{1 - \xi} \right) \left( \frac{r_c + 1}{r_c - 1} \right) \approx \frac{r_c + 1}{r_c - 1}, \quad (6)$$

$$\frac{\langle \bar{s}s \rangle}{\langle \bar{q}q \rangle} = r_c, \quad \langle \bar{q}q \rangle = \langle \bar{u}u \rangle = \langle \bar{d}d \rangle. \quad (7)$$

Furthermore, as  $\langle \bar{q}q \rangle < 0$ , if  $r_c < 1$  then  $\Psi(0) < 0$ , so the sign of the low-energy constant  $\Psi(0)$  provides valuable information on qualitative aspects of  $SU(3)$  flavor symmetry breaking by the vacuum.

There is a wide range of  $r_c$  theoretical determinations. QCD sum-rules analyses of light scalar and pseudoscalar meson correlation functions have been used to determine  $r_c$  [9,12–14], and a combined estimate from these results is  $r_c = 0.57 \pm 0.12$  [4]. QCD sum rules for baryon mass splittings tend to yield larger values ranging from the earliest determinations  $r_c = 0.8 \pm 0.1$  [15,16] to the updated values  $r_c = 0.75 \pm 0.08$  [17] and  $r_c = 0.74 \pm 0.03$  [18]. Because the QCD sum rules for heavy baryon mass splittings have better perturbative convergence compared to the light meson analyses, the most precise sum-rule value is  $r_c = 0.74 \pm 0.03$  [18]. A more conservative sum-rule value obtained from an average of light meson and baryon systems is  $r_c = 0.66 \pm 0.10$  [4]. The lattice QCD determination  $r_c = 1.08 \pm 0.16$  [19] (multiple sources of uncertainty have been combined) is considerably larger than the sum-rules determinations. An analysis combining aspects of QCD sum-rules and lattice QCD results yields  $r_c = 0.8 \pm 0.3$  [20]. The various theoretical determinations of  $r_c$  are shown in Fig. 1 and Table I.

The partially conserved axial current (PCAC) Gell-Mann-Oakes-Renner relation relates the RG invariant combination of the nonstrange quark condensate and mass parameter to pion properties [22]

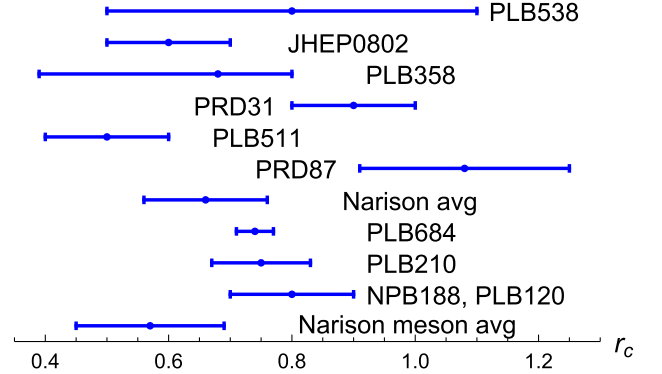


FIG. 1. Summary of  $r_c$  theoretical determinations. See Table I for key to references.

$$2m_q \langle \bar{q}q \rangle = -f_\pi^2 m_\pi^2, \quad m_q = \frac{m_u + m_d}{2}, \quad (8)$$

where in our conventions  $f_\pi = 130/\sqrt{2}$  MeV [11]. Deviations from the pion PCAC relation are bounded by approximately 5% [10,19,20] and are thus a small numerical effect. The RG invariant quark mass ratio [11]

$$r_m = \frac{m_s}{m_q} = 27.3 \pm 0.7 \quad (9)$$

can then be combined with  $r_c$  to obtain the following strange quark condensate  $m_s \langle \bar{s}s \rangle$  in terms of (8)

$$m_s \langle \bar{s}s \rangle = r_m r_c m_q \langle \bar{q}q \rangle. \quad (10)$$

A complementary approach to determinations of  $m_s \langle \bar{s}s \rangle$  is through the deviation from the kaon PCAC relation as parametrized by  $r_p$

$$-(m_s + m_u)\langle \bar{q}q + \bar{s}s \rangle \approx -m_s \langle \bar{q}q + \bar{s}s \rangle = r_p 2f_K^2 m_K^2, \quad (11)$$

where  $r_p = 1$  corresponds to the kaon PCAC result (in conventions where  $f_K = 156/\sqrt{2}$  MeV [11]) and (9) implies that neglecting  $m_u$  is a small numerical effect [see e.g., Eq. (6)]. The PCAC deviation parameter  $r_p$  can be determined in QCD sum rules by using the low-energy theorem for the pseudoscalar correlation function (3) (see e.g., Ref. [8]). A sum-rule evaluation of  $\Psi_5(0)$  thus allows determination of  $r_p$  via Eqs. (11) and (3). Significant deviations from the kaon PCAC result have been found in this approach ranging from the earliest values  $r_p = 0.63 \pm 0.08$  [8] and  $r_p = 0.5 \pm 0.17$  [21], to later determinations from Laplace sum rules  $r_p = 0.57 \pm 0.19$  [13],<sup>1</sup> QCD sum rules  $r_p = 0.66_{-0.17}^{+0.23}$  [12], lattice QCD  $r_p = 0.74 \pm 0.16$  [19], and combined approaches (merging Laplace sum

<sup>1</sup>The result of [13] has been augmented with an estimated truncation error [4].

TABLE I. Summary of  $\{r_c, r_p\}$  theoretical determinations shown in Figs. 1, 2, and 4. In some entries, multiple sources of uncertainty have been combined or ranges have been converted to an uncertainty. FESR denotes finite-energy sum-rules, LSR denotes Laplace sum rules, ChPT denotes chiral perturbation theory, QCDSR denotes QCD sum rules, AQCD denotes analytic continuation by duality, and LQCD denotes lattice QCD. The PLB511 entry includes a truncation uncertainty from Ref. [4].

$r_p$	$r_c$	Reference	Methodology
$0.56 \pm 0.16$	$0.5 \pm 0.1$	[13] (PLB511)	LSR (four loops)
$0.66^{+0.23}_{-0.17}$	$0.68^{+0.15}_{-0.29}$	[12] (PLB358)	QCDSR
$0.57 \pm 0.19$	$0.66 \pm 0.1$	[4] (Narison avg)	QCDSR average
$0.66 \pm 0.05$	$0.6 \pm 0.1$	[14] (JHEP0802)	FESR five loop
$0.39 \pm 0.22$	$0.8 \pm 0.3$	[20] (PLB538)	ChPT, LSR, and LQCD input
$0.74 \pm 0.16$	$1.08 \pm 0.16$	[19] (PRD87)	LQCD
...	$0.9 \pm 0.1$	[9] (PRD31)	LSR
...	$0.74 \pm 0.03$	[18] (PLB684)	LSR heavy baryons
...	$0.75 \pm 0.08$	[17] (PLB210)	QCDSR heavy mesons
...	$0.8 \pm 0.1$	[15,16] (NPB188, PLB120)	QCDSR baryons
...	$0.57 \pm 0.12$	[4] (Narison meson avg)	QCDSR meson average
$0.5 \pm 0.17$	...	[21] (ZPC27)	LSR, AQCD
$0.63 \pm 0.08$	...	[8] (PLB104)	QCDSR

rules, chiral perturbation theory, and lattice QCD input)  $r_p = 0.39 \pm 0.22$  [20]. The most precise determination  $r_p = 0.66 \pm 0.05$  emerges from finite-energy sum rules [14]. The various determinations of  $r_p$  are shown in Fig. 2.

The RG invariant combination of the strange quark mass and condensate emerging from the kaon PCAC relation (11) is

$$m_s \langle \bar{s}s \rangle = -r_p 2f_K^2 m_K^2 - r_m m_q \langle \bar{q}q \rangle. \quad (12)$$

The two expressions (10) and (12) for  $m_s \langle \bar{s}s \rangle$  are thus self-consistent if the following constraint is satisfied:

$$r_c = \frac{r_p}{\sigma_m} - 1, \quad (13)$$

$$\sigma_m = r_m \left( \frac{f_\pi^2 m_\pi^2}{4f_K^2 m_K^2} \right), \quad (14)$$

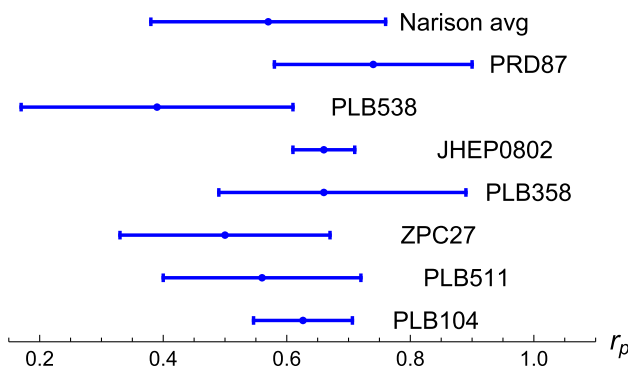


FIG. 2. Summary of  $r_p$  theoretical determinations. See Table I for key to references.

providing a correlation in the  $\{r_m, r_c, r_p\}$  parameter space. The  $\{r_c, r_p\}$  linear trajectories resulting from the PDG  $r_m$  range (9) are shown in Fig. 3. Determinations of  $r_c$  and  $r_p$  that lie along these trajectories will thus be self-consistent for the PDG range of the strange quark mass. The correlation trajectories provide a relatively more stringent constraint on  $r_p$  compared to  $r_c$ . For example, the conservative range  $0.6 < r_c < 1.2$  leads to a relatively narrow range  $0.57 < r_p < 0.86$  corresponding to a significant deviation from the kaon PCAC relation.

The most interesting analyses from the literature are those which simultaneously allow determination of both  $r_c$  and  $r_p$  because they map out a region in the  $\{r_c, r_p\}$  parameter space that can be compared with the constraint trajectories. In Fig. 4, the simultaneous determinations of  $\{r_c, r_p\}$  are compared with the linear constraint trajectories. The determinations from Refs. [4,12–14,19] show

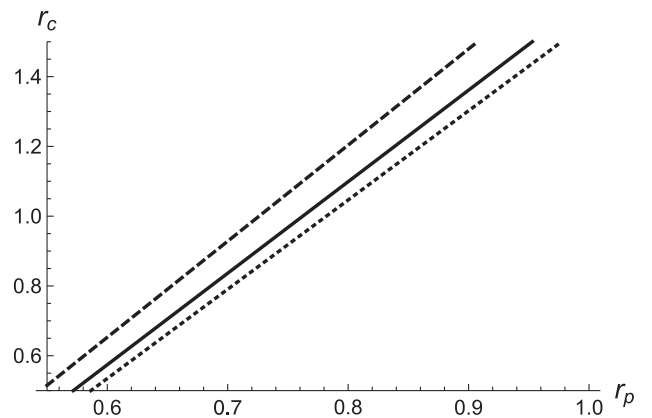


FIG. 3. Correlation (13) between  $r_p$  and  $r_c$  for PDG values [11] of  $r_m$  (solid black, dashed black, and dotted black lines respectively representing central, upper, and lower PDG values).

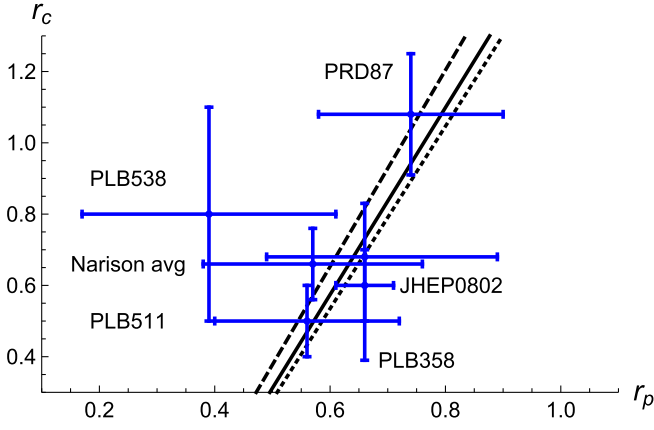


FIG. 4. Comparison of simultaneous  $\{r_p, r_c\}$  determinations with the  $\{r_p, r_c\}$  correlation trajectories (13) respectively representing central, upper, and lower PDG  $r_m$  values (solid black, dashed black, and dotted black lines). See Table I for key to references.

good agreement with the trajectories, but Ref. [20], which has the smallest determination of  $r_p$ , does not intersect the trajectories. However, Ref. [20] is somewhat different than the other simultaneous determinations in Fig. 4 because it combines different methodologies (the  $r_p$  determination in Ref. [20] involves chiral perturbation theory whereas  $r_c$  involves QCD sum rules).

As a final consideration, Fig. 5 assesses the most precise individual determinations  $r_c = 0.74 \pm 0.03$  [18] and  $r_p = 0.66 \pm 0.05$  [14] against the constraint trajectories. The two determinations delineate a compatible region of  $\{r_c, r_p\}$  parameter space, and as discussed above, the  $r_c$  determination provides a tighter bound  $0.62 < r_p < 0.69$  completely contained within the Ref. [14] determination.

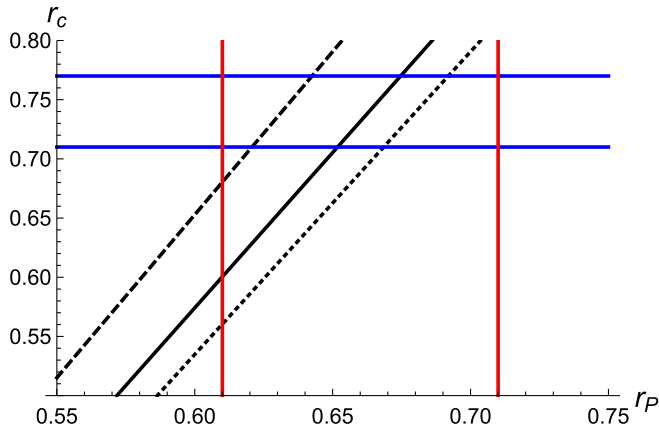


FIG. 5. Comparison of the Ref. [18]  $r_c$  bounds (blue lines) and Ref. [14]  $r_p$  bounds (red vertical lines) with the  $r_p, r_c$  correlation trajectories (13) respectively representing central, upper, and lower PDG  $r_m$  values (solid black, dashed black, and dotted black lines).

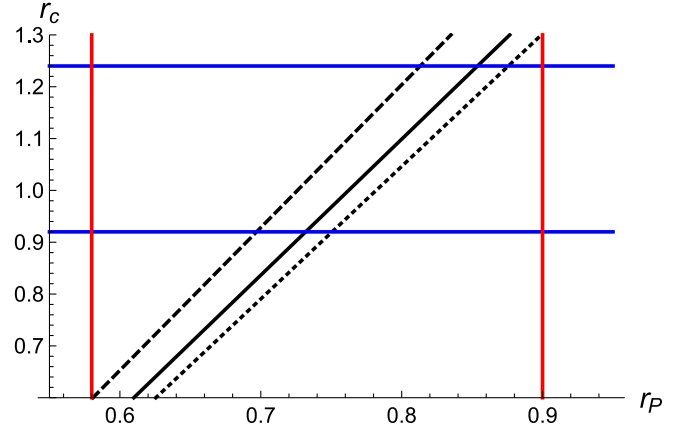


FIG. 6. Comparison of the Ref. [19]  $r_c$  bounds (blue lines) and  $r_p$  bounds (red vertical lines) with the  $r_p, r_c$  correlation trajectories (13) respectively representing central, upper, and lower PDG  $r_m$  values (solid black, dashed black, and dotted black lines).

A similar feature for the Ref. [19] lattice determinations is shown in Fig. 6; the constraint trajectories combined with the  $r_c$  determination again provide a tighter bound  $0.69 < r_p < 0.88$  completely contained within the Ref. [19] determination. Thus the constraint trajectories combined with  $r_c$  determinations tend to provide more accurate bounds on  $r_p$  than direct determinations.

Based on a small set of input parameters, we can generate a collection of self-consistent numerical results for some QCD condensates containing strange quarks. The strange quark condensate  $\langle \bar{s}s \rangle$  is often multiplied by a quark mass, *i.e.*,  $M\langle \bar{s}s \rangle$ , an RG invariant quantity. Using  $r_c = 0.74 \pm 0.03$  and (8)–(10), we find

$$m_s \langle \bar{s}s \rangle = (-1.7 \times 10^{-3}) \text{ GeV}^4. \quad (15)$$

Then, using

$$m_c \langle \bar{s}s \rangle = \left( \frac{m_c}{m_s} \right) m_s \langle \bar{s}s \rangle, \quad (16)$$

$$m_b \langle \bar{s}s \rangle = \left( \frac{m_b}{m_s} \right) m_s \langle \bar{s}s \rangle \quad (17)$$

with quark mass ratios [11]

$$\frac{m_c}{m_s} = 11.72 \pm 0.25, \quad (18)$$

$$\frac{m_b}{m_s} = 53.94 \pm 0.12, \quad (19)$$

we find

$$m_c \langle \bar{s}s \rangle = (-1.9 \times 10^{-2}) \text{ GeV}^4, \quad (20)$$

$$m_b \langle \bar{s}s \rangle = (-9.0 \times 10^{-2}) \text{ GeV}^4. \quad (21)$$

Uncertainties in (15), (20), and (21) are at most 5% and stem mainly from deviations from pion PCAC in (8). Like  $\langle \bar{s}s \rangle$ , the dimension-five mixed strange quark condensate (1) is often multiplied by a quark mass, i.e.,  $M \langle g\bar{s}\sigma Gs \rangle$ . Equations (1) and (15) give

$$m_s \langle g\bar{s}\sigma Gs \rangle = (-1.3 \times 10^{-3}) \text{ GeV}^6. \quad (22)$$

Then, again using the quark mass ratios (18) and (19), we find

$$m_c \langle g\bar{s}\sigma Gs \rangle = (-1.6 \times 10^{-2}) \text{ GeV}^6, \quad (23)$$

$$m_b \langle g\bar{s}\sigma Gs \rangle = (-7.2 \times 10^{-2}) \text{ GeV}^6. \quad (24)$$

Uncertainties in (22)–(24) are roughly 18% and stem from deviations from pion PCAC (8) and from the ratio of the strange quark condensate to the dimension-five mixed strange quark condensate in (1). Dimension-six quark condensates are often multiplied by a factor of  $\alpha_s$ . In addition, the vacuum saturation hypothesis is generally used to express dimension-six quark condensates as products of dimension-three quark condensates [1]. Using

$$\alpha_s \langle \bar{q}q \rangle^2 = 1.8 \times 10^{-4} \text{ GeV}^6 \quad (25)$$

from Ref. [2], we find with  $r_c = 0.74$  that

$$\alpha_s \langle \bar{s}s \rangle \langle \bar{q}q \rangle = 1.3 \times 10^{-4} \text{ GeV}^6, \quad (26)$$

$$\alpha_s \langle \bar{s}s \rangle^2 = 9.9 \times 10^{-5} \text{ GeV}^6. \quad (27)$$

Deviations from vacuum saturation can be applied by multiplying the results (25)–(26) by a vacuum saturation parameter  $\kappa$  where  $1 \leq \kappa \lesssim 4$  (e.g., [23,24]). Note that the result (25) is remarkably consistent with (8) and the PDG [11] values  $m_q(2 \text{ GeV}) = 3.45 \text{ MeV}$  and  $\alpha_s(2 \text{ GeV})$ .

In summary, we have developed the constraint (13) relating the strange quark parameters  $r_m = m_s/m_q$ ,  $r_c = \langle \bar{s}s \rangle / \langle \bar{q}q \rangle$  and the kaon PCAC deviation parameter  $r_p = -m_s \langle \bar{s}s + \bar{q}q \rangle / 2f_K^2 m_K^2$ . Using  $r_m$  PDG [11] values,  $\{r_c, r_p\}$  theoretical determinations (see Table I) are compared with the constraint trajectories (see Fig. 4). Theoretical predictions corresponding to the smallest value of  $r_p$  show poor agreement with the constraint trajectories. However, Fig. 5 demonstrates that the most precise values  $r_c = 0.74 \pm 0.03$  [18] and  $r_p = 0.66 \pm 0.05$  [14] are mutually consistent with the  $\{r_c, r_p\}$  constraint trajectories and provide an improved determination  $0.62 < r_p < 0.69$ . The combination of  $\{r_c, r_p\}$  constraint trajectories with  $r_c$  determinations to obtain improved  $r_p$  bounds is also observed in Fig. 6 for the lattice values [19]. Thus the  $\{r_c, r_p\}$  constraint trajectories provide a valuable methodology for assessing self-consistency or improving accuracy of determinations of the condensate ratio  $r_c = \langle \bar{s}s \rangle / \langle \bar{q}q \rangle$  and the kaon PCAC deviation parameter  $r_p = -m_s \langle \bar{s}s + \bar{q}q \rangle / 2f_K^2 m_K^2$ .

## ACKNOWLEDGMENTS

The work is supported by the Natural Sciences and Engineering Research Council of Canada (NSERC).

- 
- [1] M. A. Shifman, A. Vainshtein, and V. I. Zakharov, *Nucl. Phys.* **B147**, 385 (1979).  
 [2] M. A. Shifman, A. Vainshtein, and V. I. Zakharov, *Nucl. Phys.* **B147**, 448 (1979).  
 [3] L. J. Reinders, H. Rubinstein, and S. Yazaki, *Phys. Rep.* **127**, 1 (1985).  
 [4] S. Narison, *QCD as a Theory of Hadrons From Partons to Confinement* (Cambridge University Press, Cambridge, England, 2007), <https://doi.org/10.1017/CBO9780511535000>.  
 [5] P. Gubler and D. Satow, *Prog. Part. Nucl. Phys.* **106**, 1 (2019).  
 [6] M. Beneke and H. G. Dosch, *Phys. Lett. B* **284**, 116 (1992).  
 [7] V. Belyaev and B. Ioffe, *Sov. Phys. JETP* **56**, 493 (1982).  
 [8] S. Narison, *Phys. Lett.* **104B**, 485 (1981).  
 [9] C. A. Dominguez and M. Loewe, *Phys. Rev. D* **31**, 2930 (1985).  
 [10] C. A. Dominguez, *Quantum Chromodynamics Sum Rules* (Springer International Publishing, New York, 2018), <https://doi.org/10.1007/978-3-319-97722-5>.  
 [11] P. A. Zyla *et al.* (Particle Data Group), *Prog. Theor. Exp. Phys.* (2020), 083C01.  
 [12] S. Narison, *Phys. Lett. B* **358**, 113 (1995).  
 [13] C. A. Dominguez, A. Ramlakan, and K. Schilcher, *Phys. Lett. B* **511**, 59 (2001).  
 [14] C. A. Dominguez, N. F. Nasrallah, and K. Schilcher, *J. High Energy Phys.* **02** (2008) 072.  
 [15] B. L. Ioffe, *Nucl. Phys.* **B188**, 317 (1981); **B191**, 591(E) (1981).  
 [16] L. J. Reinders, H. R. Rubinstein, and S. Yazaki, *Phys. Lett.* **120B**, 209 (1983); **122B**, 487(E) (1983).  
 [17] S. Narison, *Phys. Lett. B* **210**, 238 (1988).  
 [18] R. M. Albuquerque, S. Narison, and M. Nielsen, *Phys. Lett. B* **684**, 236 (2010).

- [19] C. McNeile, A. Bazavov, C. T. H. Davies, R. J. Dowdall, K. Hornbostel, G. P. Lepage, and H. D. Trotter, *Phys. Rev. D* **87**, 034503 (2013).
- [20] M. Jamin, *Phys. Lett. B* **538**, 71 (2002).
- [21] C. A. Dominguez, M. Kremer, N. A. Papadopoulos, and K. Schilcher, *Z. Phys. C* **27**, 481 (1985).
- [22] M. Gell-Mann, R. Oakes, and B. Renner, *Phys. Rev.* **175**, 2195 (1968).
- [23] S. Narison, *Phys. Lett. B* **361**, 121 (1995).
- [24] R. A. Bertlmann, C. A. Dominguez, M. Loewe, M. Perrottet, and E. de Rafael, *Z. Phys. C* **39**, 231 (1988).